Supplementary data

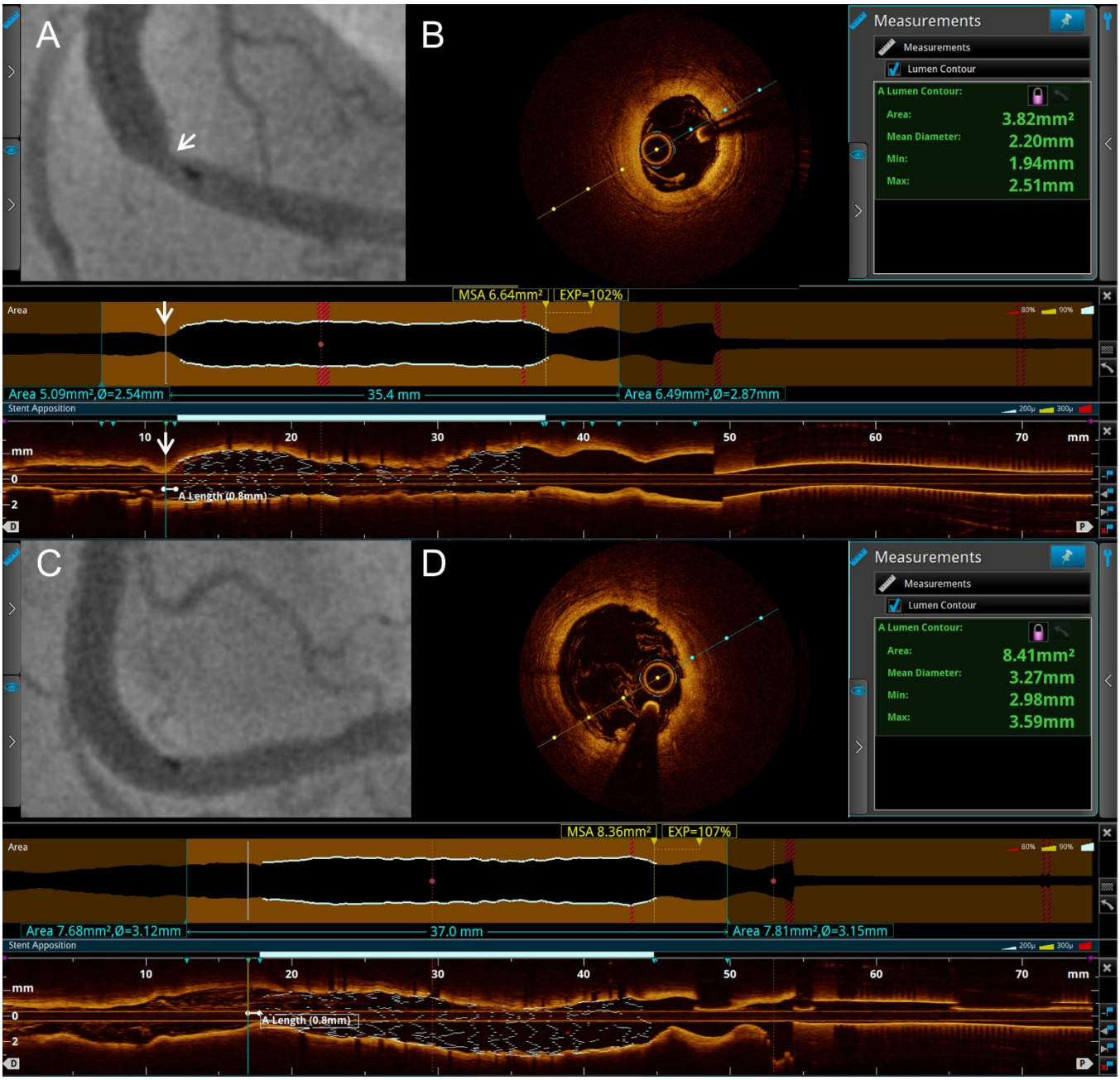

Supplementary Figure 1. Coronary artery spasm.

Following PCI optimisation, angiography (A) and OCT (B) identify severe luminal narrowing (arrowhead) at the distal stent edge with a minimal lumen area of 3.82 mm^2. Following administration of 200 mcg of intracoronary nitroglycerine, the luminal narrowing disappeared on angiography (C) and OCT (D) (arrowhead), with an improvement in the luminal area at the site of previous minimal lumen area to 8.41 mm^2.

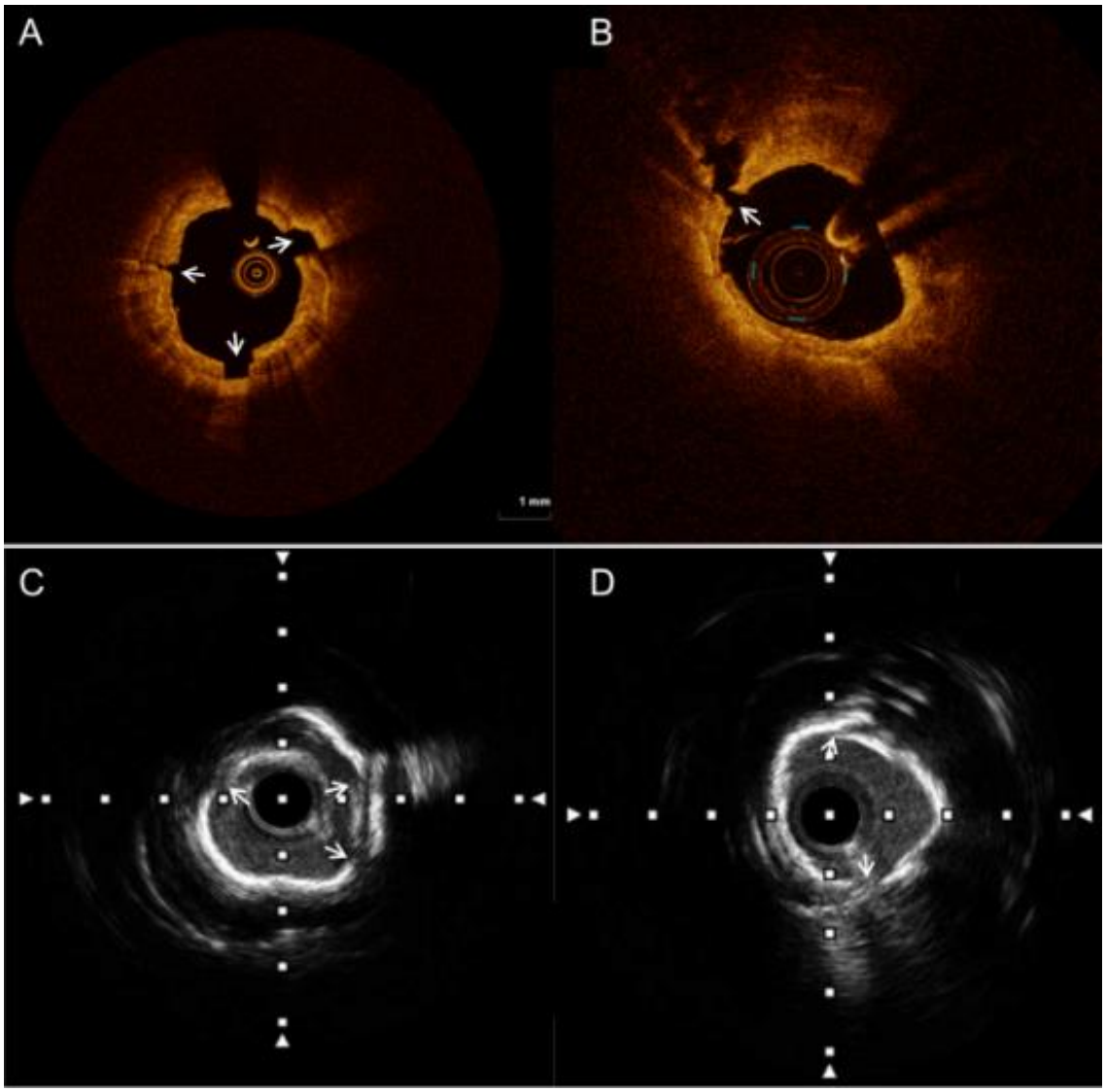

Supplementary Figure 2. Comparison of calcium fracture by OCT and HD-IVUS**.**

A) & B) Calcified plaque is visualised with low attenuation and sharply delineated borders on OCT. Arrows show calcium fracture.

C) & D) Calcified plaque on IVUS is identified as a region having a hyperechoic leading edge with acoustic shadowing. Gaps with reverberation in the hyperechoic region represent calcium fractures (arrows).

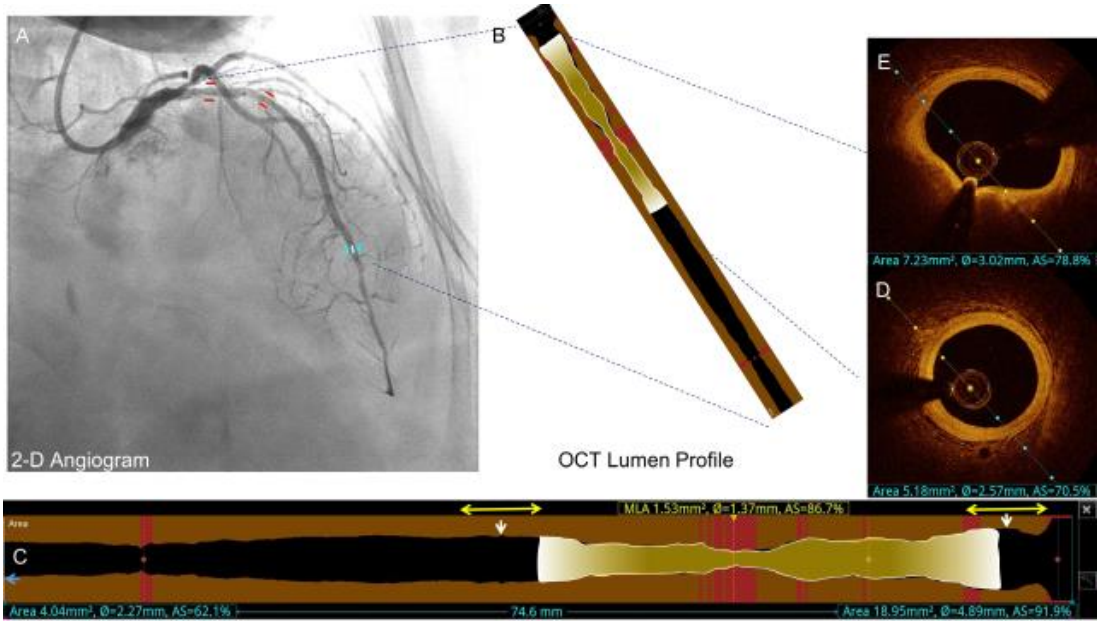

Supplementary Figure 3. Determination of lesion length on OCT.

A) Coronary angiogram represents a 2D image lumenogram of a 3D structure.

B) & C) The OCT lumen profile accounts for the 3D structure of the coronary artery lumen by incorporating mean diameter measurements as a multiplanar reconstruction. On the lumen profile, the reference vessel markers (blue arrows) are moved to the respective distal and proximal reference cross-sections, determined with the largest diameter based on visual estimation of the profile (white arrows). The cross-sections are examined as safe landing zones by assessment of the amount of visible EEL. If 360 degrees of the EEL is not visible, the segments within 5 mm proximal and distal to the chosen reference frame (yellow arrow) are perused to identify the segment with the maximal visible EEL. Finally, either the proximal or distal reference marker, whichever is on the side with greater EEL visibility, is adjusted to a commercially available DES size.

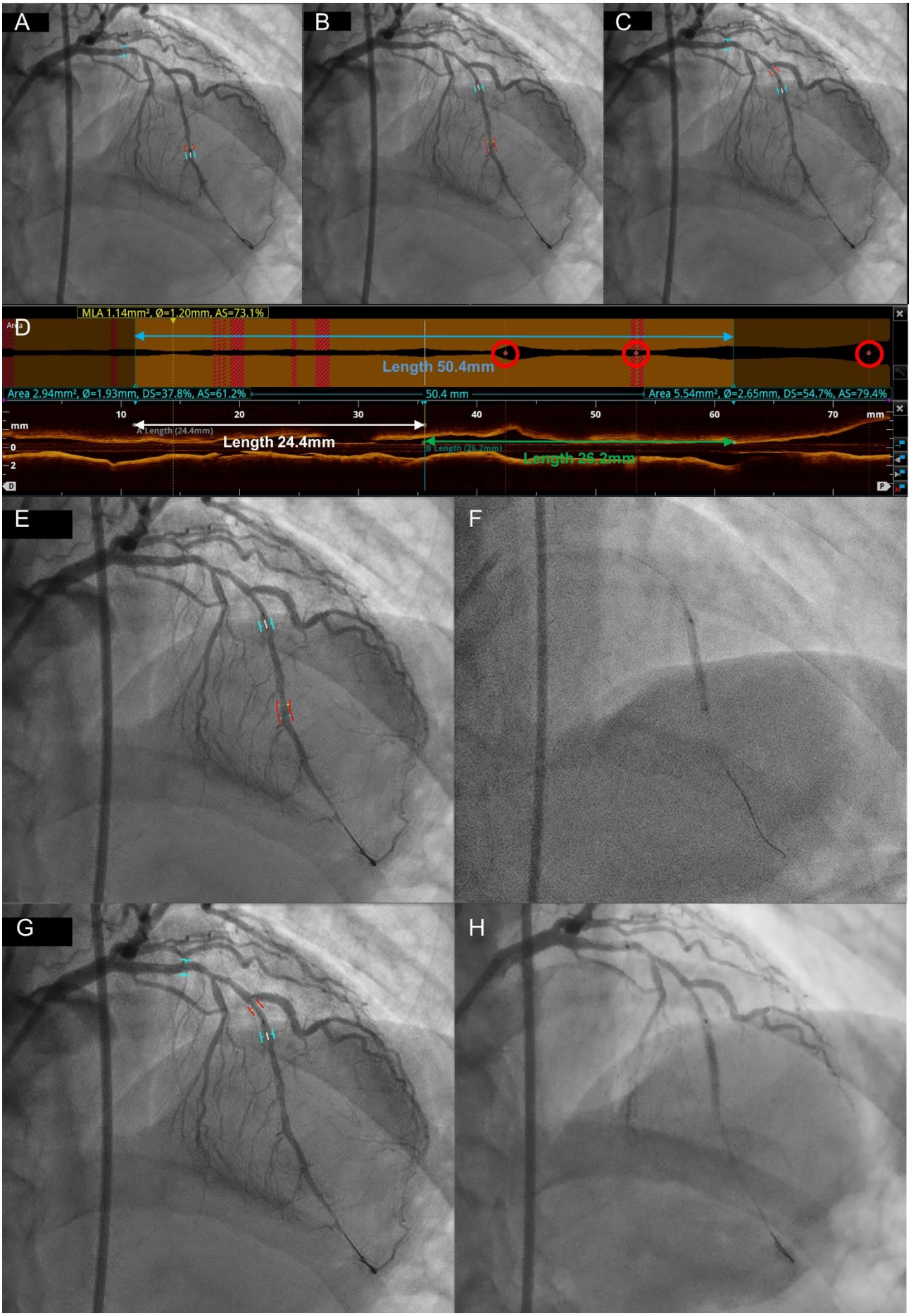
A
B
C
D
MLA 1.14mm², Ø=1.20mm, AS=73.1%
Length 50.4mm
Area 2.94mm², Ø=1.93mm, DS=37.8%, AS=61.2%
50.4 mm
Area 5.54mm², Ø=2.65mm, DS=54.7%, AS=79.4%
10
20
30
40
50
60
70
mm
A Length (24.4mm)
Length 24.4mm
B Length (26.2mm)
Length 26.2mm
E
F
G
H

Supplementary Figure 4. OCT angiographic co-registration.

A) OCT angiographic co-registration displays the reference landing zones (blue bars) in a long lesion, highlighting the total, and individual (B, C) stent lengths required.

D) On OCT lumen profile, the total stent length required is calculated to be 50.4 mm (blue arrow). The lumen profile also facilitates planning for placement of the distal (white arrow, 24.4 mm) and proximal (green arrow, 26.2 mm) devices, thus avoiding double jailing of the OCT-detected side branches (red circles).

E) The reference markers are adjusted to guide placement of the distal stent (28 mm), by aligning the OCT co-registration mark adjacent to the (F) live fluoroscopy screen.

G) The reference markers are re-adjusted to guide placement of the proximal stent (28 mm) by aligning the OCT co-registration mark adjacent to the (H) live fluoroscopy screen, confirming overlap of the two stents.

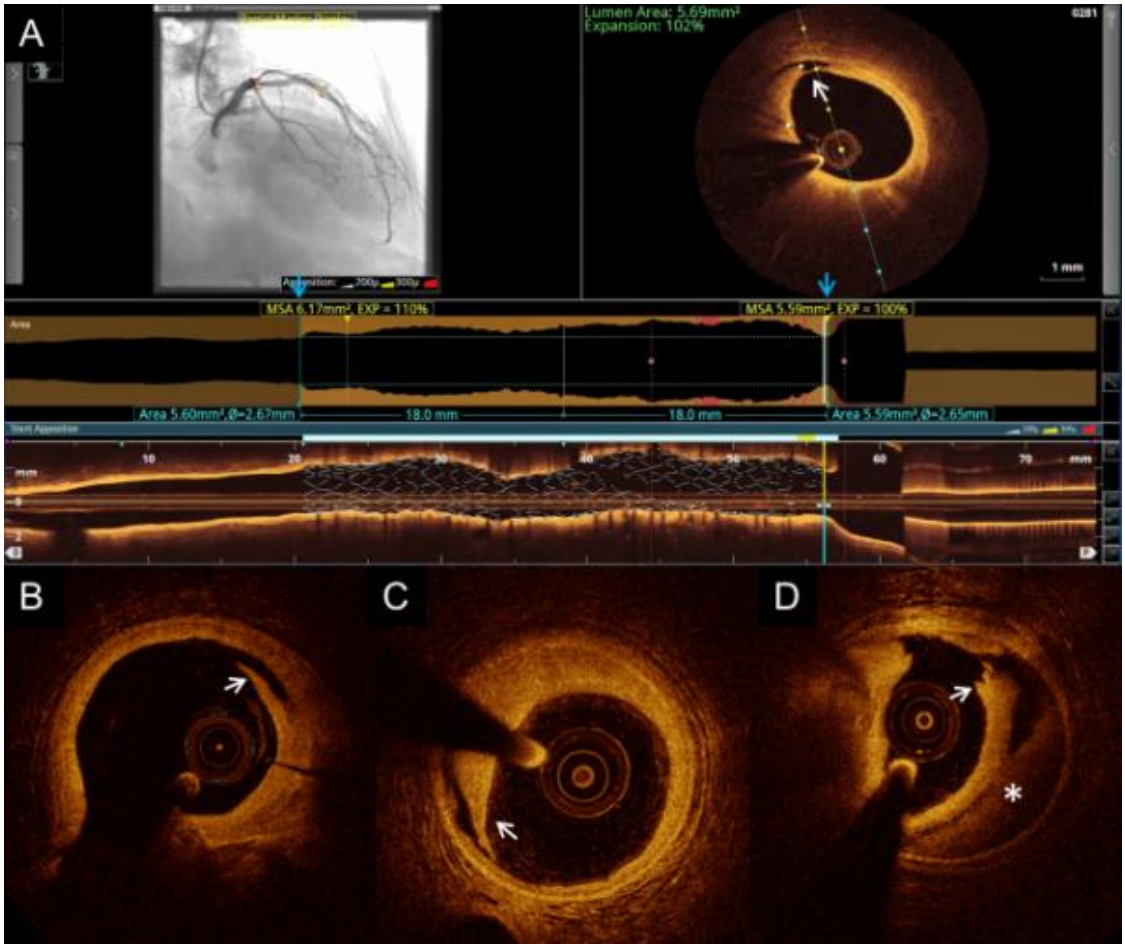

Supplementary Figure 5. Assessment of stent edge dissection on OCT.

A) Identification of the stent edge dissection (white arrow) is facilitated by automated stent rendering, allowing rapid perusal of the stent edges (blue arrows).

B) Dissections confined to the intima are considered benign as progression to intramural haematoma is rare.

C) Dissections penetrating the medial layer may progress to (D) intramural haematoma and therefore should be considered for treatment if deemed major (>1 quadrant in arc), particularly at the distal stent edge where dissection is associated with adverse events.

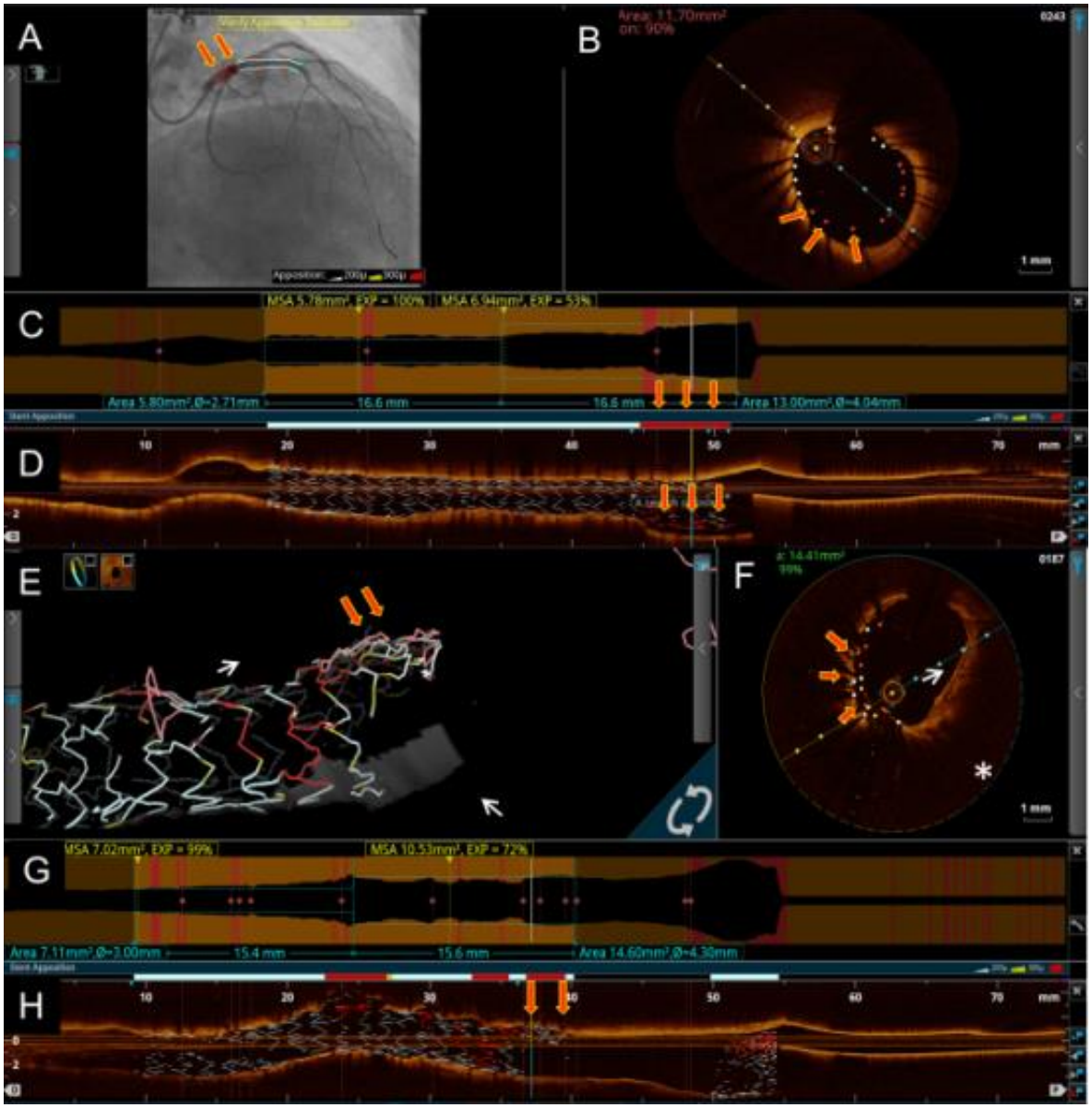

Supplementary Figure 6. Detection of stent edge malapposition by OCT.

A) Automated detection of malapposition on OCT. The high resolution of OCT allows automatic detection of malapposition. Malapposed segments and stent struts are highlighted in red in the angiographic co-registration (B), OCT cross-section (C), automated measures apposition bar (red arrows - red segments of white bar denote malapposed segments) (D) and rendered stent (red arrowheads, red stent struts of white rendered stent denote malapposed segments) on the longitudinal OCT image.
E) 3D stent rendering mode identifies the consequences of wiring through malapposed stent struts followed by balloon dilation leading to stent deformation. Malapposed segments and stent struts are highlighted in red in the 3D mode (F), OCT cross-section (G), automated measures apposition bar (red arrows - red segments of white bar denote malapposed segments) (H) and rendered stent (red arrowheads - red stent struts of white rendered stent denote malapposed segments) on the longitudinal OCT image.

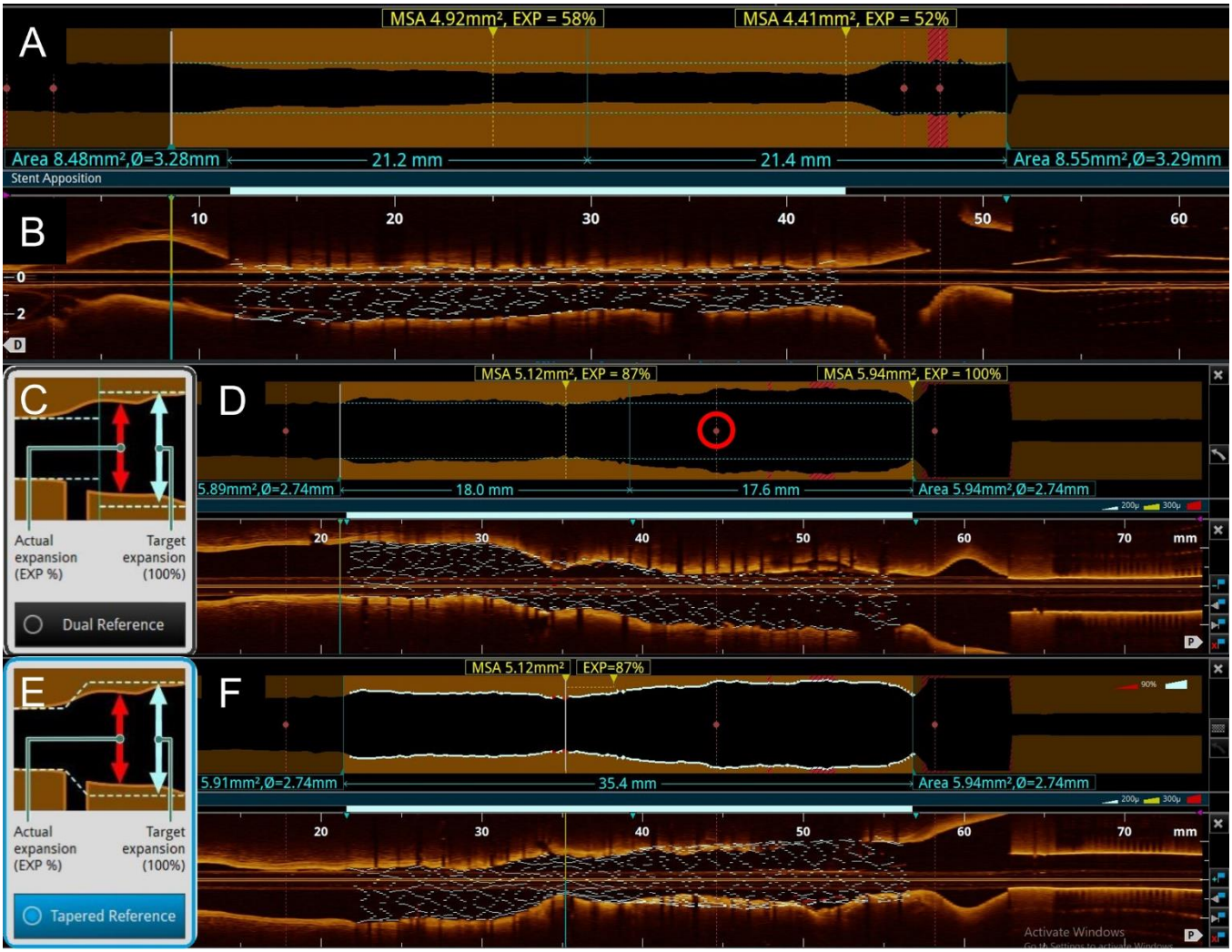

Supplementary Figure 7. Assessment of stent expansion on OCT.

A) The automated lumen profile shows stent expansion of 58% in the distal half and 52% in the proximal half of the stent (using the dual reference method). However, there is complete apposition (B) in the longitudinal OCT image (white bar), highlighting the difference between malapposition and expansion.

C) Using the dual reference mode, the stent is automatically split into two halves, (D) automatically showing an 87% expansion in the distal half, and 100% expansion in the proximal half. In the presence of a visually estimated 2.5 mm side branch, the stent should be split into segments, rather than halves, identified by the OCT automated side branch detection (red circle).

E) Using the tapered reference mode, the expansion is calculated based on interpolation of the expected tapering that occurs with side branches, (F) automatically showing an 87% expansion. Note

that the expansion in the tapered mode and the dual reference mode are the same, as the side branch had not markedly changed the interpolated reference vessel size.

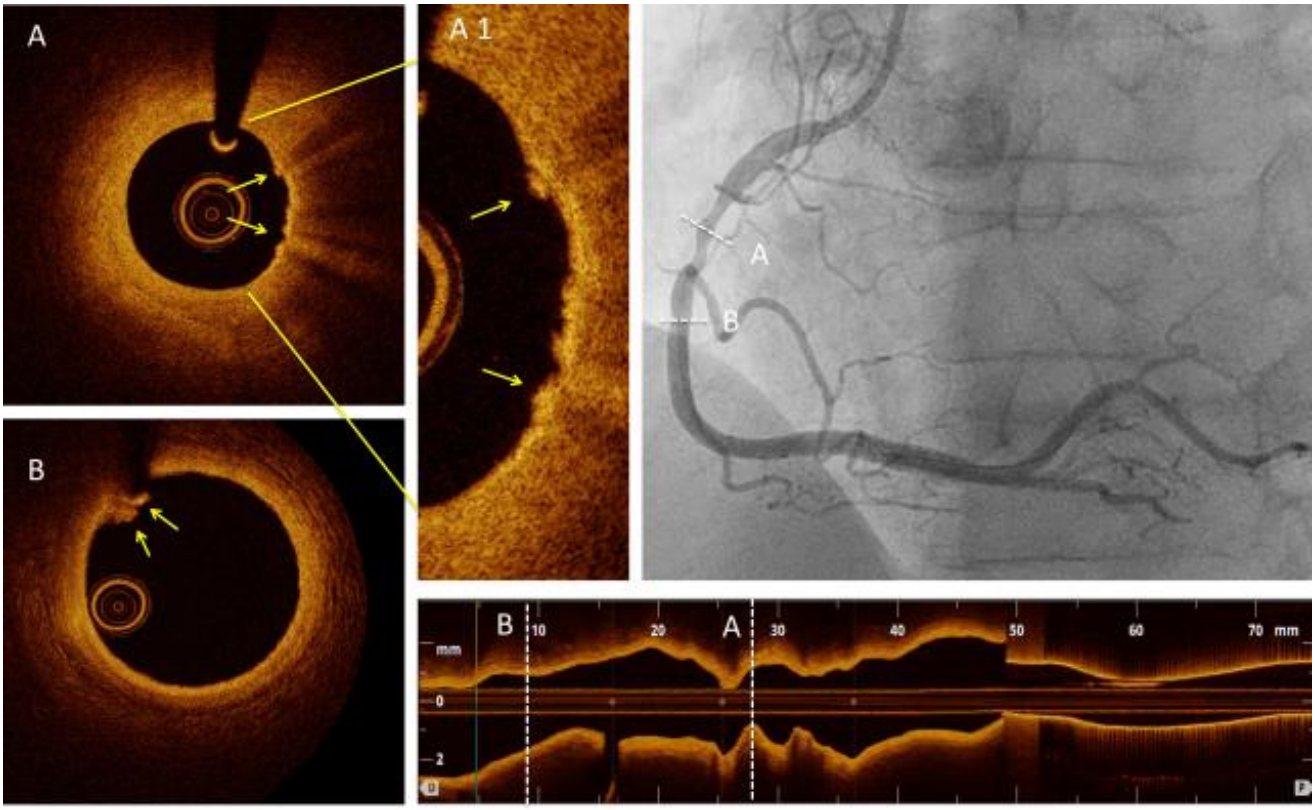

Supplementary Figure 8. Visualisation of plaque erosion in NSTEMI by OCT.

A) OCT of a moderately stenotic mid-RCA lesion identifies (A1) irregular luminal surface, suggestive of endothelial denudation (arrows).

B) OCT identifies residual thrombus in the distal reference section (arrows).

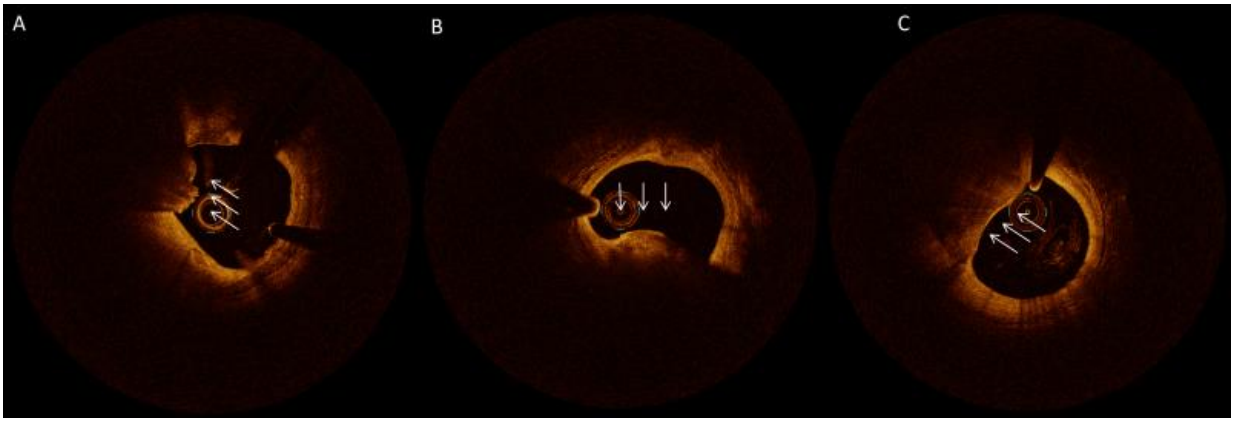

Supplementary Figure 9. Representative images of calcified plaque morphologies.

A) Eruptive calcific nodule is typically identified by a cluster of small calcific nodules protruding into the lumen.

B) Calcified protrusion is identified as a protruding calcific mass without small eruptive calcific nodules.

C) Calcific sheet is identified as sheet-like superficial calcific plate with minimal or no disruption of the overlying fibrous tissue and minimal compromise of the lumen.

A **B** **C**

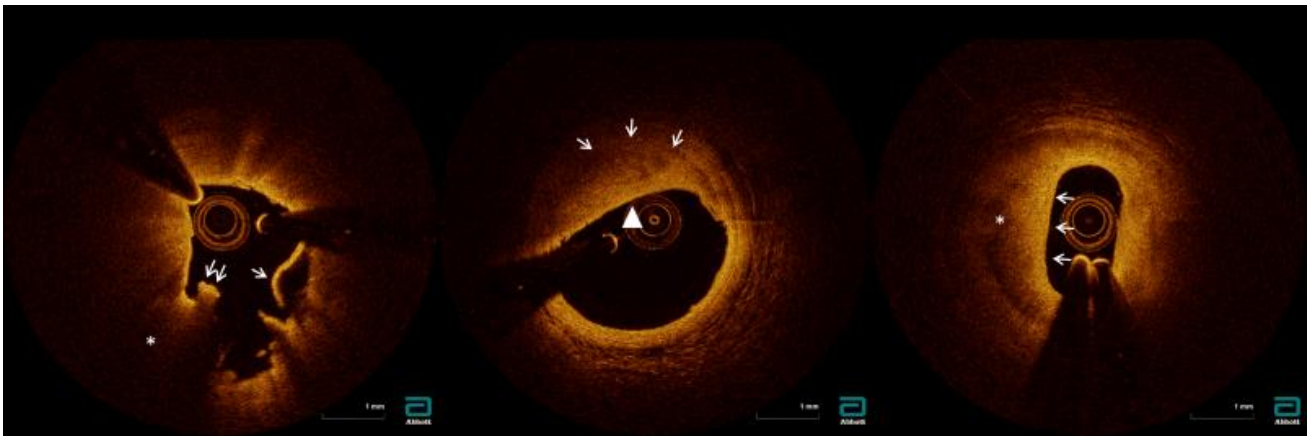

Supplementary Figure 10. Representative OCT images demonstrating common types of culprit lesions in MINOCA.

A) Plaque rupture. There is discontinuity of a thin fibrous cap (arrow), indicating plaque rupture. There is red thrombus adjacent to the rupture site (double arrow). The underlying plaque is a lipidic plaque (*).

B) Intra-plaque cavity. There are low-intensity regions with limited attenuation indicating organised thrombus and/or injected contrast in the ruptured cavity (arrowhead) overlaying a high-backscattered fibrous cap (arrows).

C) Layered plaque. There is a heterogeneous layer (arrows) overlaying a lipidic plaque (*) indicating healing of a recent plaque rupture.

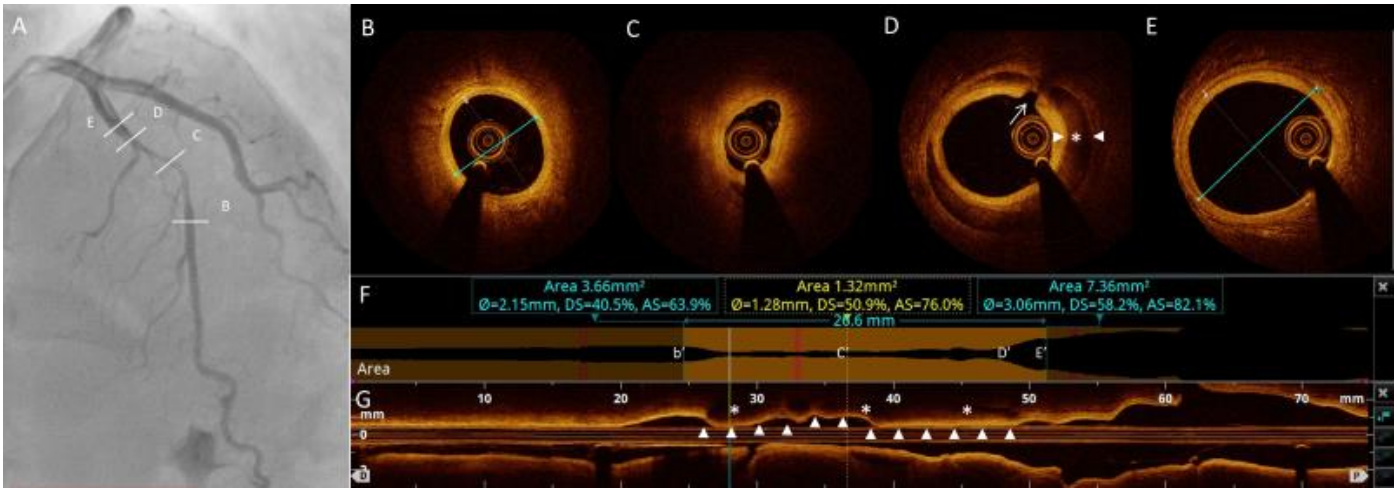

Supplementary Figure 11. Spontaneous coronary artery dissection (SCAD) on OCT.

A) Angiography identifies a luminal narrowing in the mid-LAD artery.

B) – E) OCT cross-sectional images of the distal (B) and proximal (E) segments appear as normal, while intimal disruption (arrow) and intramural haematoma (IMH, asterisk) developed inside a false lumen within the media (arrowheads) are identified (D), causing significant luminal obstruction (C).

F) The length of the dissection and diameter and area stenosis are shown on the automated longitudinal measurements while, on the longitudinal OCT image (G), the length of the affected segments (arrowheads) and extent of the IMH (asterisks) are visualised with reference to cross-sections B-E.

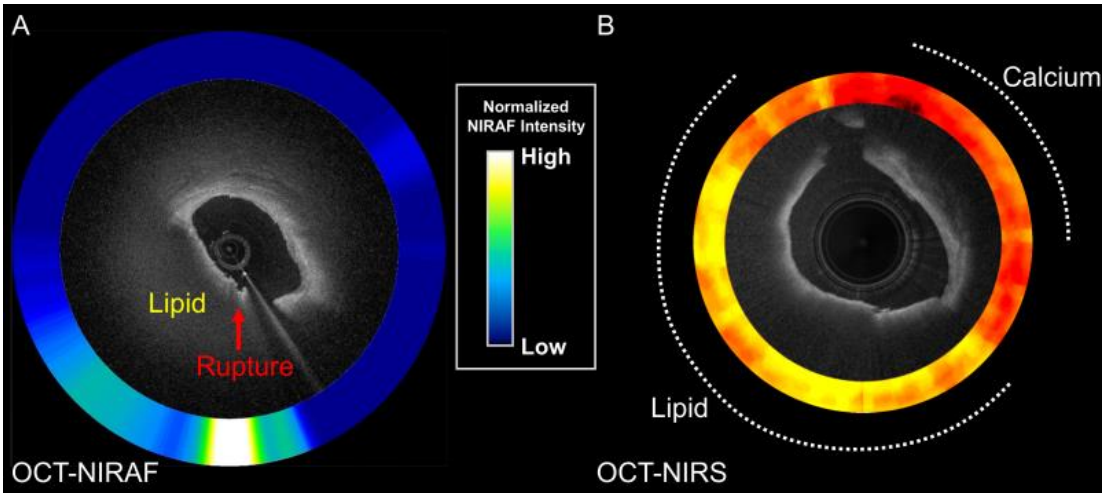

Supplementary Figure 12. Cross-sectional images of (A) OCT-near-infrared autofluorescence (NIRAF), highlighting increased NIRAF signal at the site of a plaque rupture in vivo.
B) OCT-near-infrared spectroscopy (NIRS) in a cadaver specimen, highlighting the ability of NIRS to detect lipid. Courtesy of Gary Tearney, Ali Fard, Farouc Jaffer, Giovanni Ughi.

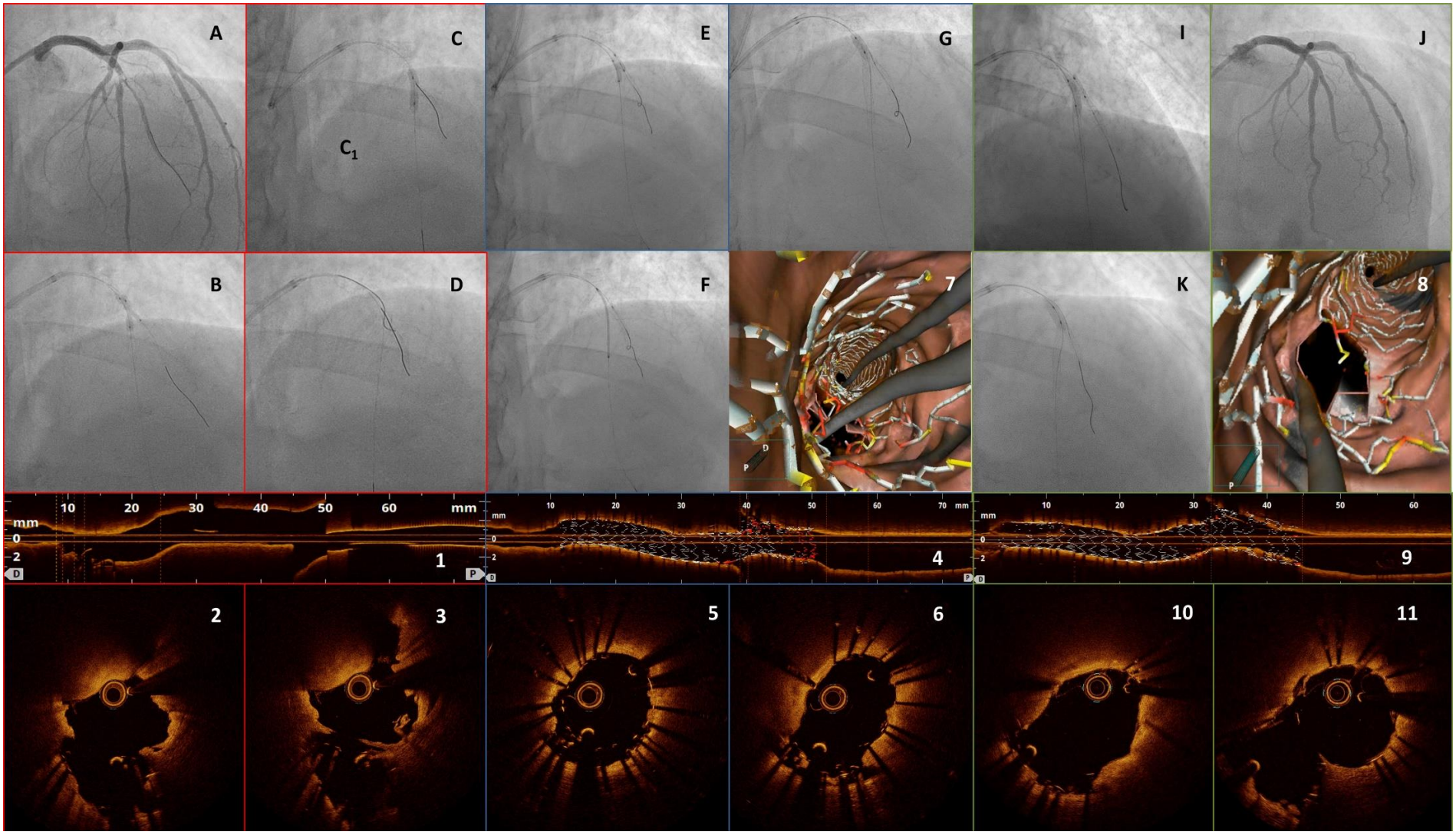
A
C
C1
E
G
I
J
B
D
F
7
K
8
10
20
30
40
50
60
mm
1
70
4
9
2
3
5
6
10
11

Supplementary Figure 13. OCT-guided double-kiss crush stenting of the LAD-D1 bifurcation.

A) Angiography identifies severe bifurcation disease at the LAD-D1 bifurcation with the angle <70°.
B) Kissing balloon inflation was used for lesion preparation, followed by (C_1) positioning of balloon in the main branch (MB) and stent in side branch (SB) and subsequent (C) crushing of the deployed SB stent with main vessel balloon inflation.
D) Rewiring of the SB was performed through the crushed SB stent struts, trying to cross the proximal cell. OCT images: (1) long-axis view of the lesion after SB stenting and rewiring, with cross-sections showing (2) wire crossing the SB stent cells (rhombus) in a proximal position, position of MB guidewire (asterisk) and (3) wire positioned in the SB stent (rhombus). Following the (E) first kissing balloon inflation between stented SB and MB vessel, (F) the MB stent was positioned in the LAD artery and deployed. Subsequently, (G) the first proximal optimisation technique (POT) and second rewiring through struts of the MB stent to the SB were performed. OCT images: (4) long-axis view after MB stenting and second rewiring with (5) wire distally crossing through MB stent cells (rhombus) and guidewire in the MB stented vessel (asterisk) with (6) wire correctly positioned in the SB stent (rhombus). (7) 3D rendering in bifurcation mode shows the architecture of the stent struts with deformation and covering of the SB ostium.
I) Second kissing balloon inflation between the stented MB and SB with (K) final POT with non-compliant balloon and (J) final angiography. OCT images: (8) 3D bifurcation mode showing opened SB struts without significant malapposition and (9) long axis with rendered stent well apposed. Cross-sections (10,11) show excellent apposition and expansion.